Coupled Systems Mechanics, *Vol. 14, No. 5 (2025) 413-429*
https://doi.org/10.12989/csm.2025.14.5.413

Nonlinear thermo-piezoelectric waves in a cracked nano-beam with non-ideal support

S. Muthulakshmi[1a], R. Selvamani*[1] and F. Ebrahimi[2]

[1]*Department of Mathematics*, *Karunya Institute of Technology and Sciences Coimbatore*, *Tamil Nadu*, *India*
[2]*Mechanical Engineering Department*, *Faculty of Engineering*, *Imam Khomeini International University*, *Qazvin*, *Iran*

(Received March 12, 2025, Revised September 3, 2025, Accepted September 23, 2025)

Abstract. This paper examines the free vibration of a cracked nano-beam with non-ideal support, considering thermo -piezoelectric effects through Euler-Bernoulli beam theory and nonlocal strain gradient theory (NSGT). A new approach models crack propagation in nano-beams using torsion springs within the NSGT framework, incorporating thermo-piezoelectric effects. The governing equations, incorporating non-ideal boundary conditions and related effects, are derived using Hamilton's method. The nano-beam is divided into two segments linked by a massless spring, accounting for additional strain energy and the deflection slope discontinuity induced by the crack. This study examines the effects of non-ideal supports, crack position, piezoelectricity, temperature variations, normal stress and strain, and the nonlocal parameter on the system's dynamic behavior. Comparisons with vibrational existing studies reveal strong agreement, emphasizing the significant impact of these parameters on characteristics.

Keywords: crack; free lateral vibration; non-ideal; nonlocal strain gradient theory; piezoelectric nano structured beam; thermal elasticity

1. Introduction

Thermo-Piezoelectric cracked nanobeams are widely used in nano sensors, actuators, and energy harvesting applications due to their ability to convert mechanical energy into electrical signals. They play a crucial role in nano-electromechanical systems (NEMS) and micro-electromechanical systems (MEMS), enabling high-precision sensing and actuation. In structural health monitoring, they help detect micro-cracks in aerospace and civil engineering structures. Their application extends to biomedical fields, where they function as nano-biosensors for detecting biological markers and in targeted drug delivery systems. Additionally, they are used in nano-robotics for precise positioning and adaptive smart materials that change properties based on external stimuli. Their unique mechanical and electrical properties make them essential for modern technological advancements. In recent years, the modeling of nanostructures has gained significant

*Corresponding author, Associate Professor, E-mail: selvam1729@gmail.com
[a]Ph.D., E-mail: smuthulakshmi0198@gmail.com

http://www.techno-press.org/?journal=csm&subpage=8 ISSN: 2234-2184 (Print), 2234-2192 (Online)

attention from researchers.

Eringen (1983) examined how integropartial differential equations from the linear theory of nonlocal elasticity can be transformed into singular partial differential equations for a specific class of physically valid kernels. Solutions were derived for both screw dislocations and surface waves. Sourki *et al.* (2016, 2017) examined the vibrations of cracked Euler-Bernoulli nanobeams, deriving governing equations using Hamilton's method based on the modified couple stress theory and examining factors affecting the natural frequency. Barretta *et al.* (2019) analyzed the static behavior of curved nanobeams using nonlocal continuum mechanics, formulating the governing equations were derived through the nonlocal integral method, with a focus on examining the influence of various parameters on the static response of the curved nanobeam.

Alizadeh Hamidi *et al.* (2022) developed the study to derive and solve the governing equation for natural frequency, analyzing the effects of nonlocal and material length scale parameters on torsional stiffness softening and hardening. Loya *et al.* (2009) analyzed the flexural vibrations of cracked micro- and nanobeams using nonlocal elasticity theory. Frequency equations were derived for various boundary conditions, taking into account the effects of crack position and length. Alwabli *et al.* (2021) studied a mechanical model of microtubule buckling using modified strain gradient theory and a new trigonometric beam theory. The formulation simplifies kinematics with only one unknown, improving efficiency. Chen *et al.* (2021) developed by This study examines the dynamic stability of FGM conical micro shells with magneto strictive face sheets under axial compression and a magnetic field, considering nonlocal and strain gradient effects Ohab-Yazdi *et al.* (2021) investigated the vibrations of functionally graded Euler-Bernoulli nano-beams with material properties varying in both longitudinal and transverse directions. The governing equations were formulated using Eringen's nonlocal theory and Hamilton's principle, and the generalized differential quadrature (GDQ) method was used for their solution. The study also analyzed the effects of various parameters on the system. Rahmani *et al.* (2015,2016) and analyzed the torsional vibrations of cracked nanobeams, modeling the crack as a torsional coil. Using Hamilton's principle and nonlocal elasticity theory, they established relationships for various boundary conditions and analyzed the impact of different parameters on the vibrational behavior of the nanobeam. Ebrahimi *et al.* (2018) analyse wave propagation in rotating FG temperature-dependent nanobeams under thermal loading using a nonlocal strain gradient model. Governing equations are derived via Hamilton's principle, and analytical solutions reveal key dispersion effects. The findings aid nanoscale machine design. Pinnola *et al.* (2021) examined the random flexural vibrations of Euler-Bernoulli nano-beams, incorporating external damping effects. After deriving the governing equations, the study analyzed the influence of various parameters on the nano-beam's flexural vibrations. Song *et al.* (2021) developed the finding that the temperature rise in thermal post buckling is more significant with strain gradient effects and no nonlocality than when nonlocality is present without strain gradient effects. Scorza *et al.* (2022) studied the mechanical behavior of cracked nanobeams using a two-phase local/nonlocal Stress-Driven Integral Model (SDM) based on Euler-Bernoulli beam theory. They also compared this model with the nonlocal strain gradient theory and analyzed the effects of different parameters on the system. Eaghbali *et al.* (2021, 2022) examined the free vibrations of a functionally graded nanobeam with an attached mass using nonlocal strain gradient theory. The study analyzed the effects of nonlocal parameters, material properties, and geometric ratios on the vibrational behavior of the nanobeam. Esen *et al.* (2022) investigated the free vibration and buckling stability of functionally graded (FG) nanobeams subjected to magnetic and thermal fields, highlighting the effects of these external factors on the structural behavior. Hao-Nan *et al.* (2021) analyzed the vibrations of rotating

functionally graded piezoelectric nanobeams, deriving the governing equations using nonlocal elasticity theory. Mahaveer Sree Jayan *et al.* (2020) investigated the wave propagation behavior of thermo elastic non-homogeneous Euler nanobeams, analyzing the impact of material inhomogeneity on wave characteristics under various boundary conditions. Zhang *et al.* (2021) stated that since these components are often used in dynamic or moving systems, achieving optimal vibrational properties and characteristics is essential for effective design. Crack propagation and growth in nanobeams using torsion spring modeling within NSGT remain unexplored. Zarepour *et al.* (2021) highlight the need for precise calculations to optimize nano-components, especially in the nano-electromechanical industry. Zhang *et al.* (2021) investigated the free vibrations of a piezoelectric nanobeam resting on a viscoelastic foundation. Using Hamilton's principle, they derived the governing equations and examined various vibration-related parameters. Sobamowo (2022) studied nonlinear vibrations of nanobeams under thermal and magnetic effects using Hamilton's principle, nonlocal theory. The Galerkin method, based on the Euler-Bernoulli beam model, was used to analyze temperature effects on vibrational frequency. Selvamani *et al.* (2020, 2023, 2024) investigated the wave propagation behavior of non-homogeneous Euler nanobeams. Their study focused on how material inhomogeneity influences wave characteristics, considering different boundary conditions. Taima *et al.* (2023) analyzed by the vibration response of cracked nanobeams considering the effects of crack length, crack position, temperature gradient, boundary conditions, and foundation stiffness, while incorporating thermal effects. With advancing science and rising demand, tools and devices are becoming lighter, smaller, and more efficient. Atci *et al.* (2017, 2021) analyzed a nanobeam with non-ideal supports using modified couple stress theory. Frequency equations were derived for various boundary conditions and weighting factors, considering the effects of crack position. Analysis on microbeams showed that non-ideal clamped boundary conditions resulted in significant decreasing of natural frequencies and shifting of stability regions. Lee (2013) developed a mathematical model based on a linear combination of ideal clamped and simply supported boundary conditions.

This paper investigates the free transverse vibrations of cracked nanobeams in a thermo-piezoelectric system under a non-ideal environment, employing Euler-Bernoulli beam theory and NSGT. The nanobeam is divided into two sections linked by a rotational spring. Using Hamilton's principle, the governing equations, boundary conditions, and thermo-piezoelectric effects are derived, along with a weighting factor representing non-ideal properties. The study explores the influence of crack depth, temperature, piezoelectric effects and the nonlocal parameter.

2. Formulation of the problem and basic equations

2.1 Nonlocal strain gradient theory

Nonlinear strain gradient theory as presented in the reference [15], stress comprises both the nonlocal elastic stress field and the strain gradient stress field.

$$t_{xx} = \sigma_{xx} - \nabla\sigma_{xx}^{(1)}. \tag{1}$$

Eq. (1), σ_{xx} represents the classical stresses, while $\sigma_{xx}^{(1)}$ correspond to the higher-order stresses [9, 15]. Additionally, in Eq. (1), $\nabla = \frac{\partial}{\partial x}$. Thus, the result is

$$[1 - (e_0 a)^2\nabla^2]t_{xx} = E(x)\varepsilon_{xx} - l^2\nabla(E(x)\nabla\varepsilon_{xx}) \tag{2}$$

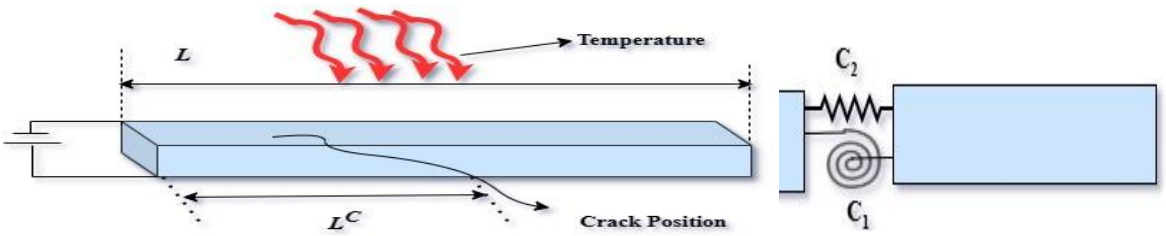

Fig. 1 Geometry of the problem

where $(e_0a)^2$ represents the nonlocal parameter and l denotes the material characteristic length.

Here a nano-beam length L, width B and height h, as shown in Fig. 1, we were connected a spring at the crack position. The governing equation for the free transverse vibration of a nano-beam, considering the effects of piezoelectric and electric influences, is derived using Hamilton's method.

2.2 Hamilton's principle

The virtual strain energy of the beam is influenced by size [9, 15]. Additionally, the virtual energy encompasses potential, kinetic, thermal, and external forces, expressed in the form of Eq. (3).

$$\begin{gathered}\delta U = \int_0^L \left(N_{xx}\delta\frac{\partial u}{\partial x} - M\delta\frac{\partial^2 w}{\partial x^2}\right)dx + \left[N_{xx}^{(1)}\delta\frac{\partial u}{\partial x} - M^{(1)}\delta\frac{\partial^2 w}{\partial x^2}\right]_0^L,\\ \delta K = \int_V \rho(x)\frac{\partial u_1}{\partial t}\delta\left(\frac{\partial u_1}{\partial t}\right)dV + \int_V \rho(x)\frac{\partial u_3}{\partial t}\delta\left(\frac{\partial u_3}{\partial t}\right)dV\\ = \int_0^L \rho(x)A\frac{\partial u}{\partial t}\delta\left(\frac{\partial u}{\partial t}\right)dx + \int_0^L \rho(x)I\frac{\partial^2 w}{\partial x\partial t}\delta\left(\frac{\partial^2 w}{\partial x\partial t}\right)dx + \int_0^L \rho(x)A\frac{\partial w}{\partial t}\delta\left(\frac{\partial w}{\partial t}\right)dx,\\ \delta F_{EX} = \int_0^L (N_P + N_E)\left(\frac{\partial w}{\partial x}\right)\delta\left(\frac{\partial w}{\partial x}\right)dx,\\ \delta \mathcal{W}_{xt} = \frac{1}{2}\int_0^L (N_T)\frac{\partial w}{\partial \theta}\delta\frac{\partial w}{\partial \theta}d\theta,\\ N_T = \int_{-\frac{h}{2}}^{\frac{h}{2}} E[Z,T]\lambda_1(Z,T)\Delta T dz.\end{gathered} \tag{3}$$

here, N_P, N_E and N_T denote the axial loads due to the piezoelectric effect, external electrostatic effect, and thermal loading, respectively, while ρ represents the material density.

The stress outcomes are obtained as

$$\begin{gathered}M^{(1)} = \int_A Z\sigma_{xx}{}^{(1)}dA\\ M = \int_A Z t_{xx}dA\\ N_{xx}^{(1)} = \int_A \sigma_{xx}^{(1)}dA\\ N_{xx} = \int_A t_{xx}dA\end{gathered} \tag{4}$$

in Eq. (4), M represents the conventional moment, while $M^{(1)}$ denotes the non-conventional

moment. Similarly, N_{xx} and $N_{xx}^{(1)}$ correspond to conventional and non-conventional force results, respectively. From Eq. (3), it is evident that the governing equation is influenced by mechanical and electric loads through the applied forces N_P and N_E.

Rotational inertia is extracted as

$$\begin{Bmatrix} A \\ I \end{Bmatrix} = b \int_{-\frac{h}{2}}^{\frac{h}{2}} \begin{Bmatrix} 1 \\ Z^2 \end{Bmatrix} dz. \tag{5}$$

This paper derives the nano beam equation using the Hamilton principle, as presented in Eq. (6)

$$\int_{t_1}^{t_2} (\delta K - \delta U + \delta F_{EX} + \delta \mathcal{W}_{xt}) dt = 0. \tag{6}$$

By solving the relationship and factorization using Eqs. (3) and (6), the stability equation and boundary conditions result in the following effect.

$$\delta U = \frac{\partial N_{xx}}{\partial x} = 0$$

$$\delta w: \frac{\partial^2 M}{\partial x^2} + \frac{\partial}{\partial x}\left(\rho(x) I \frac{\partial^3 w}{\partial x \partial t^2}\right) - \rho(x) A \frac{\partial^2 w}{\partial t^2} - (N_P + N_E)\frac{\partial^2 w}{\partial t^2} - \frac{1}{2} N_T \frac{\partial^2 w}{\partial \theta^2} = 0$$

here I denote the second moment of area, A is the cross-sectional area and $w(x, t, \theta)$ denotes the transverse displacement.

2.3 Free vibration with ideal supports

The ideal boundary conditions are

$$\begin{bmatrix} N_{xx} = 0 \\ \frac{\partial M}{\partial x} \text{ or } \delta w \\ (N_P + N_E)\left(\frac{\partial w}{\partial x}\right) \end{bmatrix}_{x=0,L} \begin{Bmatrix} M = 0 \\ N_{xx}{}^{(1)} \\ M^{(1)} \text{ or } \frac{\partial^2 w}{\partial x^2} \text{ or } \frac{\partial^2 w}{\partial \theta^2} \end{Bmatrix}. \tag{7}$$

The final equation of the Euler-Bernoulli beam method, based on strain gradient theory, is used to analyze transverse vibration as follows

$$\begin{aligned} EI\frac{\partial^4 w}{\partial x^4} - l^2 EI\frac{\partial^6 w}{\partial x^6} + \rho A\frac{\partial^2 w}{\partial t^2} - \rho I\frac{\partial^4 w}{\partial x^2 \partial t^2} - (e_0 a)^2 \rho A\frac{\partial^4 w}{\partial x^2 \partial t^2} - (N_P + N_E)\frac{\partial^2 w}{\partial x^2} + (e_0 a)^2 (N_P + \\ N_E)\frac{\partial^4 w}{\partial x^4} + (e_0 a)^2 \rho I\frac{\partial^6 w}{\partial x^4 \partial t^2} - \frac{1}{2} N_T \frac{\partial^2 w}{\partial \theta^2} + \frac{1}{2}(e_0 a)^2 (N_T)\frac{\partial^4 w}{\partial \theta^4} = 0. \end{aligned} \tag{8}$$

Where in Eq. (8)

$$N_P = P_0, N_E = 2e_{31} V_0 \tag{9}$$

in Eq. (9), V_0 represents the electrical voltage, P_0 denotes the axial force and e_{31} is the plane stress state.

Considering [25] that

$$w(x, t) = V(x) e^{i\omega t}. \tag{10}$$

Substituting Eq. (10) in Eq. (8)

$$\begin{aligned} -l^2 EIV^6(x) + (EI - (e_0 a)^2 \rho I\omega^2 + (e_0 a)^2 (N_P + N_E) + N_T) V^4(x) + (\rho I\omega^2 + \\ (e_0 a)^2 \rho A\omega^2 + (N_P + N_E) + N_T) V''(x) - \rho A\omega^2 V(x) = 0 \end{aligned} \tag{11}$$

$$\bar{V}=\frac{V}{L},\ \xi=\frac{x}{L},\ \alpha_1=\frac{e_0 a}{L},\ \alpha_2=\frac{1}{L},\ \lambda^4=\frac{\rho A L^4\omega^2}{EI},\ h^2=\frac{L^2\rho I\omega^2}{EI},\ \bar{N}_P=\frac{N_P L^2}{EI},\ \bar{N}_E=\frac{N_E L^2}{EI},\ \bar{N}_T=\frac{N_T L^2}{2EI}. \quad (12)$$

Combining Eq. (11) and Eq. (12) yields

$$-\alpha_2^2\bar{V}^6(\xi)+(1-\alpha_1^2h^2+\alpha_1^2((\bar{N}_P+\bar{N}_E)+\bar{N}_T)\bar{V}^4(\xi)+(h^2+\alpha_1^2\lambda^4+(\bar{N}_P+\bar{N}_E)+\bar{N}_T)\bar{V}''(\xi)-\lambda^4\bar{V}(\xi)=0. \quad (13)$$

Solving Eq. (13) under the consider the Eq. (14) leads to Eq. (15) as given in the reference [25]

$$\bar{V}(\xi)=\sum_{k=1}^{6}\bar{V}_k exp\,(\eta_k\xi) \quad (14)$$

$$-\alpha_2^2\eta^6+(1-\alpha_1^2h^2+\alpha_1^2((\bar{N}_P+\bar{N}_E)+\bar{N}_T)\eta^4+(h^2+\alpha_1^2\lambda^4+(\bar{N}_P+\bar{N}_E)+\bar{N}_T)\eta^2-\lambda^4=0. \quad (15)$$

This results in Eq. (15), where η is given as follows

$$\eta_1^2=-\frac{1}{3(-\alpha_2^2)}\left((1-\alpha_1^2h^2+\alpha_1^2((\bar{N}_P+\bar{N}_E)+\bar{N}_T\,)+R+\frac{(1-\alpha_1^2h^2+\alpha_1^2((\bar{N}_P+\bar{N}_E)+\bar{N}_T)^2}{R}\right),$$

$$\eta_2^2=-\frac{1}{3(-\alpha_2^2)}\left((1-\alpha_1^2h^2+\alpha_1^2((\bar{N}_P+\bar{N}_E)+\bar{N}_T)+\frac{-1-i\sqrt{3}}{2}R+\frac{(1-\alpha_1^2h^2+\alpha_1^2((\bar{N}_P+\bar{N}_E)+\bar{N}_T)^2}{\left(\frac{-1-i\sqrt{3}}{2}\right)R}\right), \quad (16)$$

$$\eta_3^2=-\frac{1}{3(-\alpha_2^2)}\left((1-\alpha_1^2h^2+\alpha_1^2((\bar{N}_P+\bar{N}_E)+\bar{N}_T)+\frac{-1+i\sqrt{3}}{2}R+\frac{(1-\alpha_1^2h^2+\alpha_1^2((\bar{N}_P+\bar{N}_E)+\bar{N}_T)^2}{\left(\frac{-1+i\sqrt{3}}{2}\right)R}\right).$$

where in Eq. (16)

$$R=2(1-\alpha_1^2h^2+\alpha_1^2((\bar{N}_P+\bar{N}_E)+\bar{N}_T)^3+\sqrt{-27(-\alpha_2^2)^2\Delta}$$
$$\Delta=-4(1-\alpha_1^2h^2+\alpha_1^2((\bar{N}_P+\bar{N}_E)+\bar{N}_T)^3(h^2+\alpha_1^2\lambda^4-\lambda^4+((\bar{N}_P+\bar{N}_E)+\bar{N}_T)-27(-\alpha_2^2)^2(h^2+\alpha_1^2\lambda^4-\lambda^4+((\bar{N}_P+\bar{N}_E)+\bar{N}_T)^2. \quad (17)$$

The third root is always physically negative and results in imaginary values, therefore

$$\bar{V}(\xi)=A_1+A_2\xi+A_3\,sinh(\eta_1\xi)+A_4\,cosh(\eta_1\xi)+A_5\,sin(\eta_2\xi)+A_6\,cos(\eta_2\xi). \quad (18)$$

2.4 Free vibrations with non-ideal support

In engineering, nanostructures are generally modelled with classical boundary condition, assuming ideal manufacturing. However, fabrication complexities can cause deviations from ideal boundary conditions, significantly affecting the dynamic properties of fabricated nanocantilevers [5].

This study examines non-ideal supports to incorporate physical effects. To illustrate their impact, clamped-clamped (c-c), simply supported (s-s), and clamped-simply supported (c-s) boundary conditions are analyzed. The following presents the mathematical model for non-ideal supports [14].

$$\bar{w}\,(\bar{x})=0, k\bar{w}(\bar{x})\pm(1-k)\bar{w}'(\bar{x})=0 \qquad 0\le k\le 1 \quad (19)$$

here k represents the weighting factor, serving as the coefficient of the non-ideal property. The

presence of the rotational term alters the classical clamped support condition into a non-classical one. Similarly, the classical simply supported boundary condition can be modified into a non-ideal form by adjusting the weighting factor of the moment effect term in the same equation. The sign switches to minus at the left edge boundary and to plus at the right edge boundary. Additionally, the classical clamped support equation is recovered by setting $k = 0$ in Eq. (19), while the classical simply supported condition is obtained by assigning $k = 1$.

To implement the conditions of non-ideal supports, Eq. (18) and its derivatives, $V'(x)$ and $V''(x)$ are substituted into Eq. (19) using the assumed solution of $w(x,t) = V(x)e^{i\omega t}$. The resulting equations are then expressed in a coefficient matrix form.

$$\begin{bmatrix} 1 & 0 & 0 & 1 & 0 & 1 \\ 0 & -(1-k) & -(1-k)\eta_1 & k{\eta_1}^2 & -(1-k)\eta_2 & -k{\eta_2}^2 \\ 1 & 1 & sinh\eta_1 & cosh\eta_1 & sin\eta_2 & cos\eta_2 \\ 0 & 1-k & k{\eta_1}^2 sinh\eta_1 + (1-k)\eta_1 cosh\eta_1 & k{\eta_2}^2 cosh\eta_1 + (1-k)\eta_1 sinh\eta_1 & -k{\eta_2}^2 sin\eta_2 + (1-k)\eta_1 cos\eta_2 & k{\eta_2}^2 cos\eta_2 + (1-k)\eta_2 sin\eta_2 \end{bmatrix} \tag{20}$$

By setting the determinant of the coefficient matrix in Eq. (20) to zero, the dimensionless natural frequencies (λ^4) corresponding to the fundamental vibration modes are determined. Additionally, the coefficients A_1, A_2, A_3, A_4, A_5, A_6 in Eq. (18) are solved using non-ideal supports to derive the modal shape function and obtain the mode shapes.

Left and Right ends are

$$\begin{gathered} V(0) = 0\,, \quad kV''(0) - (1-k)V'(0) = 0 \\ V(1) = 0, V''(1) + (1-k)V'(1) = 0. \end{gathered} \tag{21}$$

3. Crack nanobeam model

A beam with an extended edge crack is examined, where the crack is positioned at intervals of L^c starting from the left end, with a corresponding defined dimension as $b = \frac{L^c}{L}$ To incorporate the effect of crack illustrated in Fig. 1, the crack portion was removed, resulting in two separate sections connected by a massless spring at the crack position. The springs are incorporated to account for the additional pressure energy resulting from the presence of the crack [16].

The supplementary strain energy, denoted as $\Delta\psi_c$, is attributed to the crack and can be expressed as [15]

$$\Delta\psi_c = \frac{1}{2}M\Delta\theta \tag{22}$$

where $\Delta\theta$ represents the rotation angle of the rotational spring. The dimensionless form of Eq. (19) is given by

$$\Delta\theta = \frac{k_{MM}}{L}\frac{\partial^2\bar{V}}{\partial x^2}\Big|_{\xi=L^c} = K\frac{\partial^2\bar{V}}{\partial x^2}\Big|_{\xi=L^c} \tag{23}$$

where k_{MM} represents flexibility constants [16].

With the crack modeling established, the free cross-sectional vibration analysis of the beam can proceed by applying the motion equation in the vertical direction to each of the two sections.

$$\begin{gathered} -\alpha_2^2\bar{V}^6(\xi) + (1 - \alpha_1^2h^2 + \alpha_1^2((\bar{N}_P + \bar{N}_E) + \bar{N}_T)\bar{V}^4(\xi) + (h^2 + \alpha_1^2\lambda^4 + (\bar{N}_P + \bar{N}_E) + \\ \bar{N}_T)\bar{V}''(\xi) - \lambda^4\bar{V}(\xi) = 0 \qquad 0 \le \xi \le b, \end{gathered}$$

$$-\alpha_2^2\bar{V}^6(\xi)+(1-\alpha_1^2h^2+\alpha_1^2(\bar{N}_P+\bar{N}_E)+\bar{N}_T)\bar{V}^4(\xi)+(h^2+\alpha_1^2\lambda^4+(\bar{N}_P+\bar{N}_E)+\bar{N}_T)\bar{V}''(\xi)-\lambda^4\bar{V}(\xi)=0 \quad b\le\xi\le 1 \tag{24}$$

where λ^4 is the natural frequency.

The overall solution for each section can be expressed as follows

$$\begin{gathered}\bar{V}_1(\xi)=A_1+A_2\xi+A_3\,sinh(\eta_1\xi)+A_4\,cosh(\eta_1\xi)+A_5\,sin(\eta_2\xi)+A_6\,cos(\eta_2\xi)\\ 0\le\xi\le b,\\ \bar{V}_2(\xi)=B_1+B_2\xi+B_3\,sinh(\eta_1\xi)+B_4\,cosh(\eta_1\xi)+B_5\,sin(\eta_2\xi)+B_6\,cos(\eta_2\xi)\\ b\le\xi\le 1.\end{gathered} \tag{25}$$

The equations above contain multiple constants that need to be determined by applying the boundary conditions and the conditions defined at the crack section. The boundary conditions are formulated as follows [25, 26].

$$\bar{V}_1(0)=\bar{V}_1''(0)=\bar{V}_1^4(0)=0 \tag{25a}$$

$$\bar{V}_2(1)=\bar{V}_2''(1)=\bar{V}_2^4(1)=0 \tag{25b}$$

$$\begin{gathered}\bar{V}_2^4(b)=\bar{V}_1^4(b)\\ \bar{V}_2''(b)+\bar{V}_2(b)=\bar{V}_1''(b)+\bar{V}_1(b)\\ \bar{V}_2'(b)-\bar{V}_1'(b)=k\bar{V}_1''(b)\\ \bar{V}_2^5(b)=\bar{V}_1^5(b)\\ \bar{V}_2^3(b)=\bar{V}_1^3(b)\\ \bar{V}_2'(b)=\bar{V}_1'(b).\end{gathered} \tag{25c}$$

By applying the boundary conditions and the compliance conditions in Eq. (25) can be written in the matrix form

$$\begin{bmatrix}
0 & 1 & 0 & 1 & 0 & 0 & 0 & 0 & 0 & 0\\
1 & 0 & 1 & 0 & -\eta_2^2 & 0 & 0 & 0 & 0 & 0\\
0 & 0 & \eta_1^2 & 0 & \eta_2^2 & 0 & 0 & 0 & 0 & 0\\
0 & 0 & \eta_1^4 & 0 & \eta_2^4 & 0 & 0 & sinh(\eta_1) & cosh(\eta_1) & sin(\eta_2) & cos(\eta_2)\\
0 & 0 & 0 & 0 & 0 & 1 & 1 & \eta_1^2 sinh(\eta_1) & \eta_1^2 cosh(\eta_1) & -\eta_2^2 sin(\eta_2) & \eta_2^2 cos(\eta_2)\\
0 & 0 & 0 & 0 & 0 & 0 & 0 & \eta_1^4 sinh(\eta_1) & \eta_1^4 cosh(\eta_1) & \eta_2^4 sin(\eta_2) & \eta_2^4 cos(\eta_2)\\
0 & 0 & -\eta_1^4 sinh(\eta_1 b) & -\eta_1^4 cosh(\eta_1 b) & -\eta_2^4 sin(\eta_2 b) & -\eta_2^4 cos(\eta_2 b) & 0 & 0 & 0 & 0 & 0\\
0 & 0 & -(1+\eta_1^2)sinh(\eta_1 b) & -(1+\eta_1^2)cosh(\eta_1 b) & -(1-\eta_1^2)sin(\eta_1 b) & -(1-\eta_1^2)cos(\eta_1 b) & 1 & b(1+\eta_1^2)sinh(\eta_1 b) & (1+\eta_1^2)cosh(\eta_1 b) & (1-\eta_1^2)sin(\eta_1 b) & (1-\eta_1^2)cos(\eta_1 b)\\
-1 & -b & -1\eta_1 cosh(\eta_1 b)+k\eta_1^2 sinh(\eta_1 b) & \eta_1 sinh(\eta_1 b)+k\eta_1^2 cosh(\eta_1 b) & -\eta_2 cos(\eta_2 b)+k\eta_2^2 sin(\eta_2 b) & \eta_2 sin(\eta_2 b)+k\eta_2^2 cos(\eta_2 b) & 0 & 1 & \eta_1 cosh(\eta_1 b) & \eta_1 sinh(\eta_1 b) & \eta_2 cos(\eta_2 b) & \eta_2 sin(\eta_2 b)\\
0 & 0 & -\eta_1^5 cosh(\eta_1 b) & -\eta_1^5 sinh(\eta_1 b) & -\eta_2^5 cos(\eta_2 b) & \eta_2^5 sin(\eta_2 b) & 0 & 0 & \eta_1^5 cosh(\eta_1 b) & \eta_1^5 sinh(\eta_1 b) & \eta_2^5 cos(\eta_2 b) & -\eta_2^5 sin(\eta_2 b)\\
0 & 0 & -\eta_1^3 cosh(\eta_1 b) & -\eta_1^3 sinh(\eta_1 b) & \eta_2^3 cos(\eta_2 b) & -\eta_2^3 sin(\eta_2 b) & 0 & 1 & \eta_1^3 cosh(\eta_1 b) & \eta_1^3 sinh(\eta_1 b) & -\eta_2^3 cos(\eta_2 b) & \eta_2^3 sin(\eta_2 b)\\
0 & -1 & -\eta_1 cosh(\eta_1 b) & -\eta_1 sinh(\eta_1 b) & -\eta_2 cos(\eta_2 b) & \eta_2 sin(\eta_2 b) & & & \eta_1 cosh(\eta_1 b) & \eta_1 sinh(\eta_1 b) & \eta_2 cos(\eta_2 b) & -\eta_2 sin(\eta_2 b)
\end{bmatrix} \tag{26}$$

4. Numerical results and discussion

The output in this portion is derived for natural frequencies using Euler-Bernoulli beam and non-local strain gradient theory, considering various nonlocal parameters, crack position, temperature, normal stress and normal strain. The characteristics of nanobeam materials are $\rho = 8166$ (kgm^3), $E = 207$ GPa, $\frac{L}{h} = 20$.

Figs. 2 and 3 illustrate the influence of the nonlocal parameter on the frequency response of the nanobeam. A detailed analysis of these figures reveals a strong inverse relationship between the nonlocal parameter and frequency, meaning that as the nonlocal parameter increases, the frequency decreases. This trend highlights the significant role of small-scale effects in

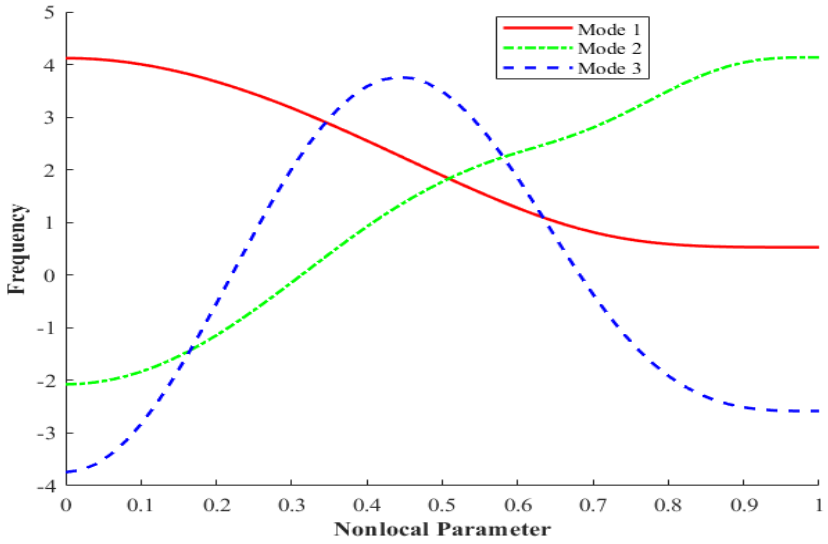

Fig. 2 Variation of frequency verses nonlocal parameter at $\eta = 0.3$

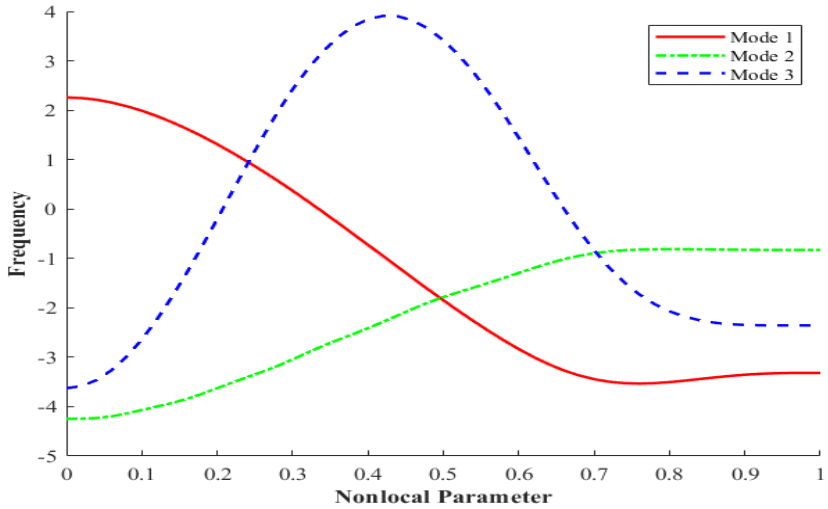

Fig. 3 Variation of frequency verses nonlocal parameter at $\eta = 0.5$

nanostructures, where increasing nonlocality leads to a reduction in the beam's stiffness, thereby lowering its natural frequency. Such behavior is particularly important in nanoscale applications, as it underscores the necessity of accounting for nonlocal effects when predicting vibrational characteristics.

Figs. 4 and 5 provide a detailed illustration of how temperature influences the frequency of the system. In these cases, the analysis is conducted for three different modes under varying temperature parameter. The results clearly indicate that as the thermal parameter (temperature) increases, there is a corresponding decrease in the beam's frequency. This trend suggests that thermal effects play a significant role in altering the dynamic behavior of the beam, likely due to changes in material properties such as stiffness and thermal expansion. The reduction in frequency

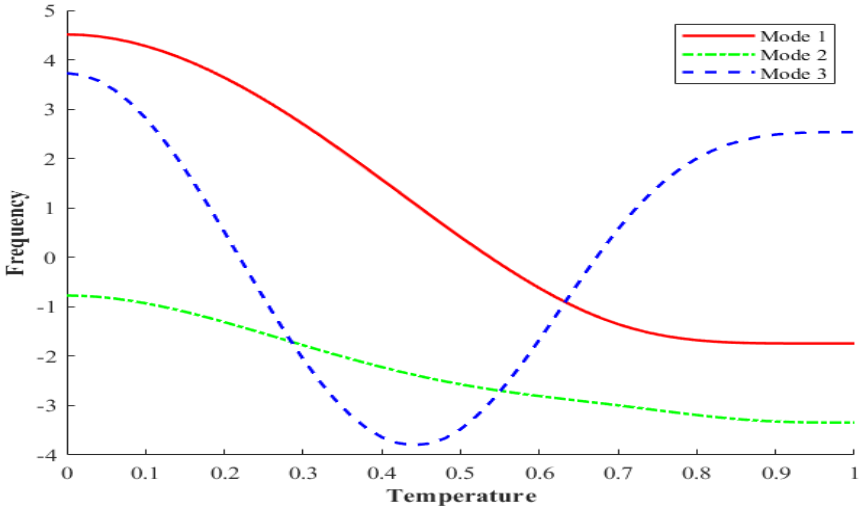

Fig. 4 Variation of frequency verses temperature at $\eta = 0.3$.

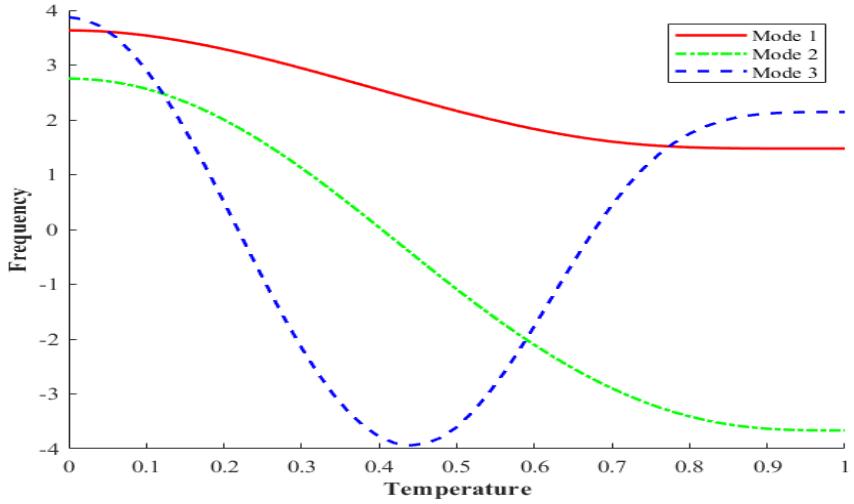

Fig. 5 Variation of frequency verses temperature at $\eta = 0.5$

with increasing temperature highlights the need for careful consideration of thermal effects in structural and mechanical applications, where temperature variations could impact performance and stability.

Figs. 6 and 7 illustrate the effect of crack position ($\eta = 0.3, 0.5$) on frequency. The results indicate that as the crack position increases, the frequency decreases. Additionally, the first and third modes of the beam with a central crack exhibit higher frequencies compared to those with a lateral crack. This suggests that cracks located closer to the beam's center have a less detrimental effect on frequency reduction than those positioned laterally.

Figs. 8 and 9 illustrate the effect of crack position ($\eta = 0.3,0.5$) on displacement, showing that as the crack position increases, the displacement decreases. This trend suggests that the structural integrity is influenced by the crack's location, with displacement being more significant when the

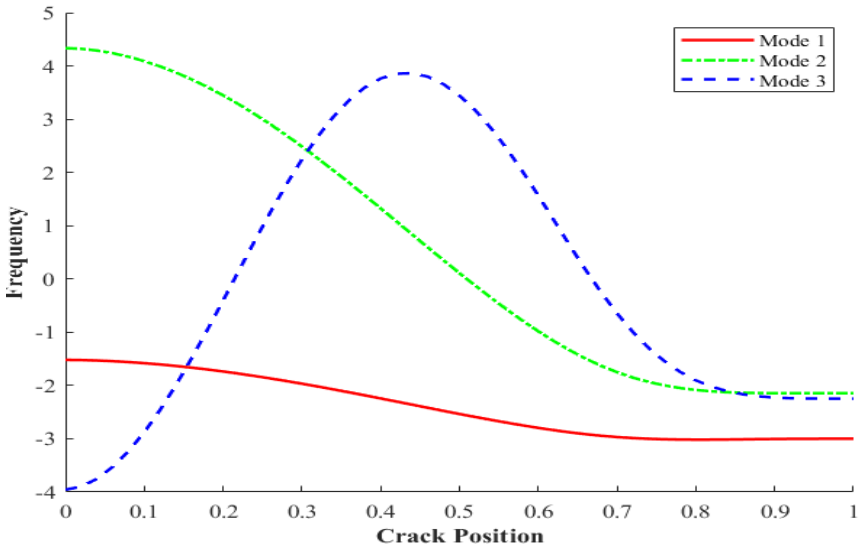

Fig. 6 Variation of frequency verses crack position at $\eta = 0.3$

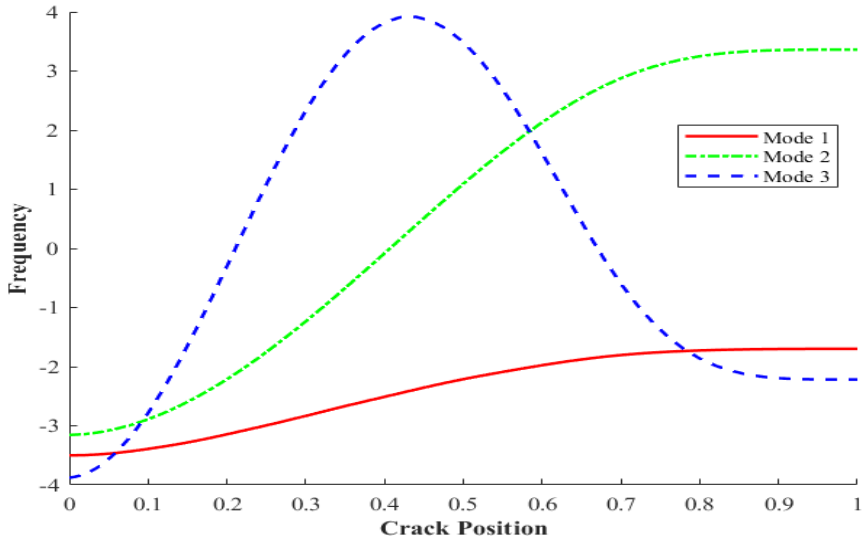

Fig. 7 Variation of frequency verses crack position at $\eta = 0.5$

crack is positioned closer to the initial reference point. The analysis is conducted for three different modes, each representing distinct loading and boundary conditions, accounting for variations in stress distribution, strain energy release, and deformation behavior under different displacement conditions. Additionally, the results indicate that as the crack moves toward the center ($\eta = 0.5$), the reduction in displacement is more pronounced, implying that crack location plays a crucial role in determining overall stiffness and deformation characteristics. These findings contribute to a better assessment of crack-induced damage and provide insights into optimizing structural design to mitigate the effects of cracks on mechanical performance.

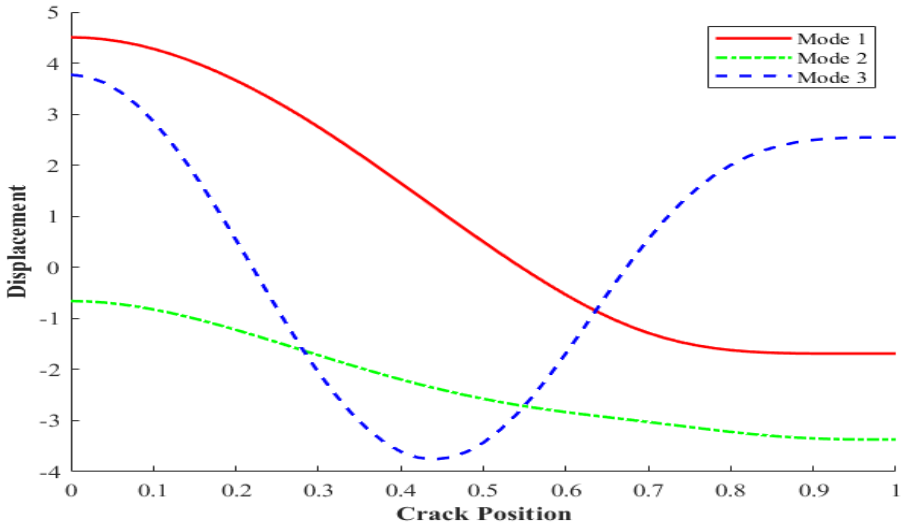

Fig. 8 Variation of displacement verses crack position at $\eta = 0.3$

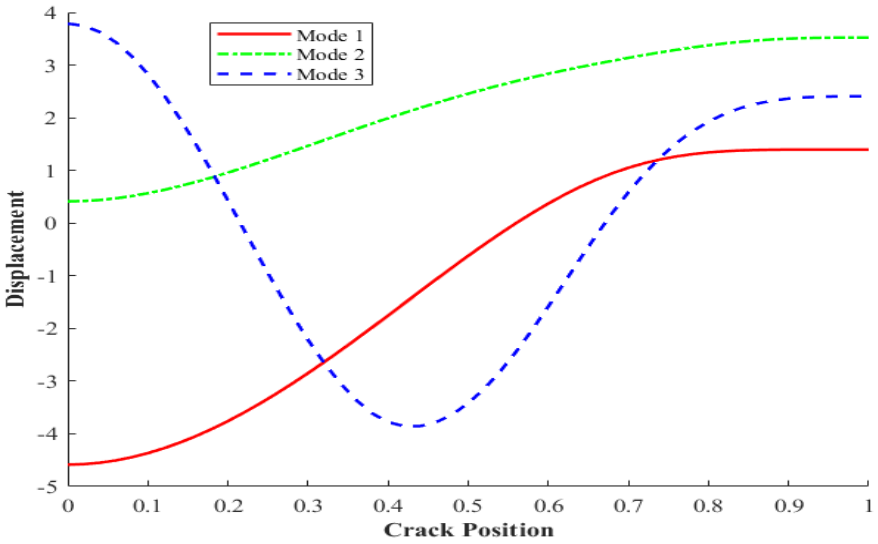

Fig. 9 Variation of displacement verses crack position at $\eta = 0.5$

Figs. 10 and 11 depict the normal strain distribution in a cracked nanobeam at different crack positions. The results clearly indicate that as the crack moves further along the beam, the normal strain experiences a reduction. This suggests that the location of the crack significantly influences the strain behavior, with higher strain values observed when the crack is positioned closer to the initial reference point. The decrease in normal strain with increasing crack position implies that the structural response of the nanobeam becomes less sensitive to deformation as the crack shifts. These findings provide valuable insights into how crack positioning affects the mechanical behavior of nanobeams, which can be useful in structural analysis and design optimization to improve durability and performance.

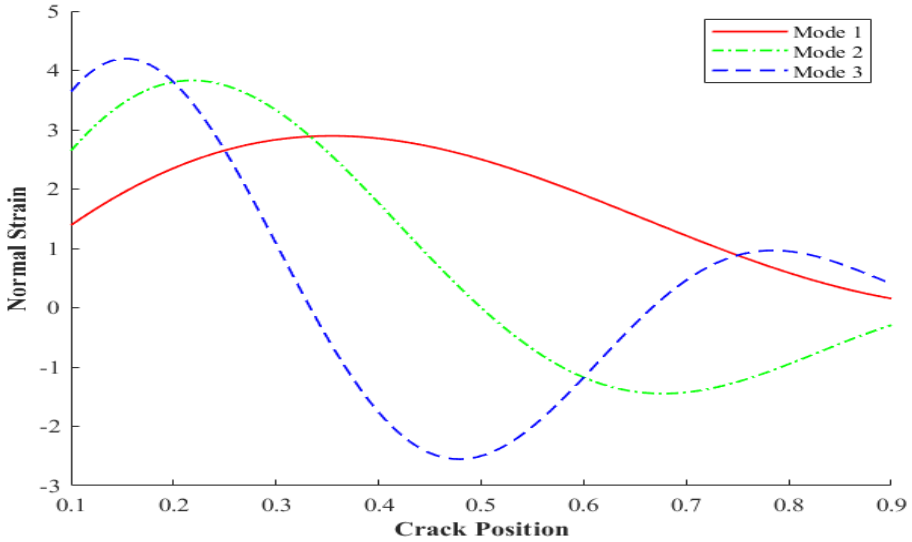

Fig. 10 Variation of normal strain verses crack position at $\eta = 0.3$

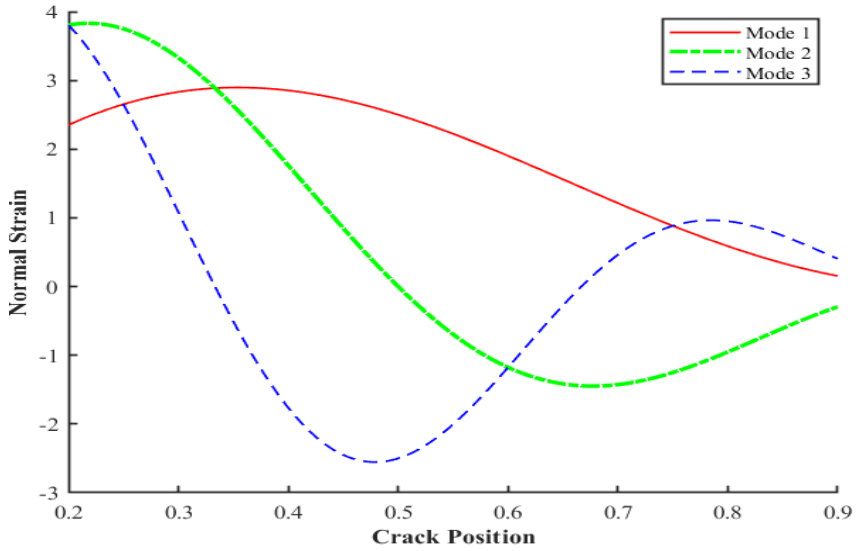

Fig. 11 Variation of normal strain verses crack position at $\eta = 0.5$

Figs. 12 and 13 show the normal stress distribution in a cracked nanobeam with varying crack positions. These figures clearly illustrate that as the crack position increases, the normal stress decreases. Additionally, the analysis reveals that Mode 2 exhibits the highest normal stress compared to the other modes. This indicates that the stress distribution is significantly influenced by the crack location and the mode of deformation, with Mode 2 experiencing the greatest stress concentration. Understanding this behavior is crucial for assessing the structural integrity of nanobeams and optimizing their design to enhance performance and durability.

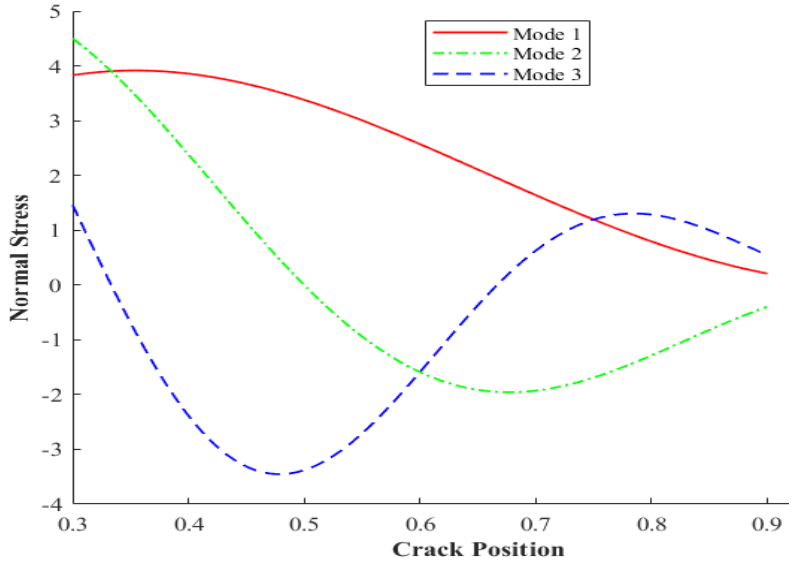

Fig. 12 Variation of normal stress verses crack position at $\eta = 0.3$

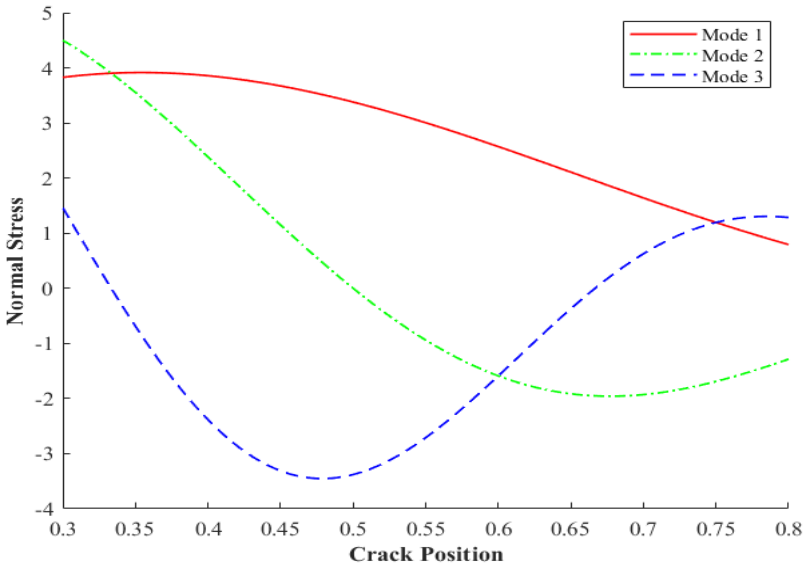

Fig. 13 Variation of normal stress verses crack position at $\eta = 0.5$

5. Conclusions

This study investigates the free vibration behavior of a cracked nano-beam using Euler-Bernoulli beam theory, incorporating strain gradient theory and considering electric voltage and thermo-piezo effects with non-ideal support. The research presents analytical solutions and numerical findings to analyze how nonlocal parameters, temperature, and crack position influence frequency, displacement, normal stress, and normal strain. Results indicate that increasing the

nonlocal parameter decreases frequency, suggesting reduced beam stiffness and highlighting the importance of nonlocal effects in nanoscale vibrations. Similarly, increasing temperature reduces the beam's frequency, affecting its dynamic behavior due to changes in material properties. The study also shows that frequency reduce as the crack position shifts along the beam, with centrally located cracks having a smaller impact on frequency reduction compared to lateral ones. Displacement decreases as the crack moves, particularly near the center, while normal strain and normal stress in the cracked nanobeam decrease as the crack position increases along the beam. These findings emphasize the sensitivity of nano-scale beam systems to material, geometric, and external field parameters, providing valuable insights for optimizing nanobeam design in terms of stability, performance, and durability in nano-electromechanical systems.

References

Alizadeh Hamidi, B., Khosravi, F., Hosseini, S.A. and Hassannejad, R. (2022), "Closed form solution for dynamic analysis of rectangular nanorod based on nonlocal strain gradient", *Wave. Random Complex Media*, **32**(5), 2067-2083. https://doi.org/10.1080/17455030.2020.1843737.

Alwabli, A.S., Kaci, A., Bellifa, H., Bousahla, A.A., Tounsi, A., Alzahrani, D.A., Abulfaraj, A.A., Bourada, F., Benrahou, K.H., Tounsi, A. and Mahmoud, S.R. (2021), "The nano scale buckling properties of isolated protein microtubules based on modified strain gradient theory and a new single variable trigonometric beam theory", *Adv. Nano Res.*, **10**(1), 15-24. https://doi.org/10.12989/anr.2021.10.1.015.

Atcı, D. (2021), "Free vibrations of nanobeams under non-ideal supports based on modified couple stress theory", *Zeitschrift für Naturforschung A*, **76**(5), 427-434. https://doi.org/10.1515/zna-2020-0335.

Atcı, D. and Bagdatlı, S.M. (2017), "Free vibrations of fluid conveying microbeams under non-ideal boundary conditions", *Steel Compos. Struct.*, **24**(2), 141-149. https://doi.org/10.12989/scs.2017.24.2.141.

Atcı, D. and Bagdatlı, S.M. (2017), "Vibrations of fluid conveying microbeams under non-ideal boundary conditions", *Microsyst. Technol.*, **23**, 4741-4752. https://doi.org/10.1007/s00542-016-3255-y.

Barretta, R., De Sciarra, F.M. and Vaccaro, M.S. (2019), "On nonlocal mechanics of curved elastic beams", *Int. J. Eng. Sci.*, **144**, 103140. https://doi.org/10.1016/j.ijengsci.2019.103140.

Chen, S.X., Sahmani, S. and Safaei, B. (2021), "Size-dependent nonlinear bending behavior of porous FGM quasi-3D microplates with a central cutout based on nonlocal strain gradient isogeometric finite element modelling", *Eng. Comput.*, **37**, 1657-1678. https://doi.org/10.1007/s00366-021-01303-z.

Ebrahimi, F. and Haghi, P. (2018), "A nonlocal strain gradient theory for scale-dependent wave dispersion analysis of rotating nanobeams considering physical field effects", *Couple. Syst. Mech.*, **7**(4), 373-393. https://doi.org/10.12989/csm.2018.7.4.373.

Eghbali, M., Hosseini, S.A. and Pourseifi, M. (2022), "Free transverse vibrations analysis of size-dependent cracked piezoelectric nano-beam based on the strain gradient theory under mechanic-electro forces", *Eng. Anal. Bound. Elem.*, **143**, 606-612. https://doi.org/10.1016/j.enganabound.2022.07.006.

Eghbali, M., Hosseini, S.A. and Rahmani, O. (2021), "Free vibration of axially functionally graded nanobeam with an attached mass based on nonlocal strain gradient theory via new ADM numerical method", *Amirkabir J. Mech. Eng.*, **53**(2), 1-8. https://doi.org/10.1080/23311916.2022.2098654.

Eringen, A.C. (1983), "On differential equations of nonlocal elasticity and solutions of screw dislocation and surface waves", *J. Appl. Phys.*, **54**(9), 4703-4710. https://doi.org/10.1063/1.332803.

Esen, I., Abdelrhmaan, A.A. and Eltaher, M.A. (2022), "Free vibration and buckling stability of FG nanobeams exposed to magnetic and thermal fields", *Eng. Comput.*, **38**(4), 3463-3482. https://doi.org/10.1007/s00366-021-01389-5.

Hao-nan, L., Cheng, L., Ji-ping, S. and Lin-quan, Y. (2021), "Vibration analysis of rotating functionally graded piezoelectric nanobeams based on the nonlocal elasticity theory", *J. Vib. Eng. Technol.*, **9**, 1155-1173. https://doi.org/10.1007/s42417-021-00288-9.

Lee, J. (2013), "Free vibration analysis of beams with non-ideal clamped boundary conditions", *J. Mech. Sci. Technol.*, **27**, 297-303. https://doi.org/10.1007/s12206-012-1245-2.

Lim, C.W., Zhang, G. and Reddy, J. (2015), "A higher-order nonlocal elasticity and strain gradient theory and its applications in wave propagation", *J. Mech. Phys. Solid.*, **78**, 298-313. https://doi.org/10.1016/j.jmps.2015.02.001.

Loya, J., Lopez-Puente, J., Zaera, R. and Fernandez-Saez, J. (2009), "Free transverse vibrations of cracked nanobeams using a nonlocal elasticity model", *J. Appl. Phys.*, **105**(4), 044309. https://doi.org/10.1063/1.3068370.

Mahaveer Sree Jayan, M., Kumar, R., Selvamani, R. and Rexy, J. (2020), "Nonlocal dispersion analysis of a fluid conveying thermo elastic armchair single walled carbon nanotube under moving harmonic excitation", *J. Solid Mech.*, **12**(1), 189-203. https://doi.org/10.22034/jsm.2019.1867399.1431.

Ohab-Yazdi, S.M.K. and Kadkhodayan, M. (2021), "Application of bi-directional functionally graded material model for free vibration analysis of rotating Euler-Bernoulli nanobeams", *Mech. Adv. Compos. Struct.*, **8**(2), 389-399. https://doi.org/10.22075/macs.2021.21231.1300.

Pinnola, F.P., Vaccaro, M.S., Barretta, R. and Marotti de Sciarra, F. (2021), "Random vibrations of stress-driven nonlocal beams with external damping", *Mechanica*, **56**, 1329-1344. https://doi.org/10.1007/s11012-020-01181-789.

Rahmani, O., Hosseini, S.A.H. and Hayati, H. (2016), "Frequency analysis of curved nano-sandwich structure based on a nonlocal model", *Mod. Phys. Lett. B*, **30**(10), 1650136. https://doi.org/10.1142/S0217984916501360.

Rahmani, O., Hosseini, S.A.H., Noroozi Moghaddam, M.H. and Fakhari Golpayegani, I. (2015), "Torsional vibration of cracked nanobeam based on nonlocal stress theory with various boundary conditions: An analytical study", *Int. J. Appl. Mech.*, **7**(03), 1550036. https://doi.org/10.1142/S1758825115500362.

Scorza, D., Luciano, R. and Vantadori, S. (2022), "Fracture behavior of nanobeams through two-phase local/nonlocal stress-driven model", *Compos. Struct.*, **280**, 114957. https://doi.org/10.1016/j.compstruct.2021.114957.

Selvamani, R., Loganathan, R., Dimitri, R. and Tornabene, F. (2023), "Nonlocal state-space strain gradient wave propagation of magneto Thermo piezoelectric functionally graded nanobeam", *Curv. Layer. Struct.*, **10**(1), 20220192. https://doi.org/10.1515/cls-2022-0192.

Selvamani, R., Mahaveer Sree Jayan, M. and Ebrahimi, F. (2020), "Ultrasonic waves in a single walled armchair carbon nanotube resting on nonlinear foundation subjected to thermal and in plane magnetic fields", *Couple. Syst. Mech.*, **10**(1), 39-60. https://doi.org/10.12989/csm.2021.10.1.039.

Selvamani, R., Mahesh, S. and Ebrahimi, F. (2021), "Frequency characteristics of a multiferroic Piezoelectric/LEMV/CFRP/Piezomagnetic composite hollow cylinder under the influence of rotation and hydrostatic stress", *Couple. Syst. Mech.*, **10**(2), 185-198. https://doi.org/10.12989/csm.2021.10.2.185.

Sobamowo, M.G. (2022), "Analysis of nonlinear vibration of piezoelectric nanobeam embedded in multiple layers elastic media in a thermo-magnetic environment using iteration perturbation method", *J. Solid Mech.*, **14**(2), 221-251. https://doi.org/10.22034/jsm.2021.1911067.1648.

Song, R., Sahmani, S. and Safaei, B. (2021), "Isogeometric nonlocal strain gradient quasi-three-dimensional plate model for thermal post buckling of porous functionally graded microplates with central cutout with different shapes", *Appl. Math. Mech.*, **42**(6), 771-786. https://doi.org/10.1007/s10483-021-2725-7.

Sourki, R. and Hoseini, S.A.H. (2016), "Free vibration analysis of size-dependent cracked microbeam based on the modified couple stress theory", *Appl. Phys. A*, **122**(4), 413. https://doi.org/10.1007/s00339-016-9961-6.

Sourki, R. and Hosseini, S.A. (2017), "Coupling effects of nonlocal and modified couple stress theories incorporating surface energy on analytical transverse vibration of a weakened nanobeam", *Eur. Phys. J. Plus*, **132**(4), 184. https://doi.org/10.1140/epjp/i2017-11488-3.

Taima, M.S., El-Sayed, T.A. and Friswell, M.I. (2023), "Thermal vibration analysis of cracked nanobeams submerged in elastic foundations by nonlocal continuum mechanics", *Thin Wall. Struct.*, **193**, 111249. https://doi.org/10.1016/j.tws.2023.111249.

Zarepour, M., Hosseini, S.A. and Kokaba, M.R. (2017), "Electro-thermo-mechanical nonlinear free

vibration of nanobeam resting on the Winkler Pasternak foundations based on nonlocal elasticity using differential transform method", *Microsyst. Technol.*, **23**, 2641-2648. https://doi.org/10.1007/s00542-016-2935-y.

Zhang, D., Liu, M., Wang, Z. and Lei, Y. (2021), "Thermo-electro-mechanical vibration of piezoelectric nanobeams resting on a viscoelastic foundation", *J. Phys.: Conf. Ser.*, **1759**, 012029. https://doi.org/10.1088/1742-6596/1759/1/012029.

Zhang, L., Guo, J. and Xing, Y. (2021), "Bending analysis of functionally graded one-dimensional hexagonal piezoelectric quasicrystal multilayered simply supported nanoplates based on nonlocal strain gradient theory", *Acta Mechanica Solida Sinica*, **34**, 237-251. https://doi.org/10.22034/jsm.2021.1911067.1648.